

Boundary Dynamics of Sweeping Interface

Hiizu Nakanishi

Department of Physics, Kyushu University 33, Fukuoka 812-8581, Japan

A new type of boundary dynamics is proposed to describe the interface that sweeps space to collect distributed material. Based upon geometrical consideration on a simple physical process representing a certain experiment, the dynamics is formulated as the small diffusion limit of Mullins-Sekerka problem of crystal growth. It is demonstrated that a steadily extending finger solution exists for a finite range of propagation speed, but numerical simulations suggest they are unstable and the interface shows a complex time development.

PACS numbers: 45.70.Qj, 81.10.Aj, 47.54.+r

I. INTRODUCTION

The boundary dynamics has been providing interesting problems for physics and mathematics. A famous one is the problem of crystal growth from a supercooled melt[1]; As the melt is solidified and a crystal grows, a flat interface between the solid and the liquid phases becomes unstable due to the coupling of the solidification process with the diffusion of latent heat generated at the interface (Mullins-Sekerka instability[2]). This results in the fascinating variety of dendritic growths of crystal under the interplay with anisotropic surface tension. Another example is the viscous fingering, which appears when the air is injected into a viscous fluid (Saffman-Taylor instability [3, 4]). The viscous fluid is displaced by the pressure gradient, and the pressure field is governed by Laplace equation with proper boundary conditions. Since Laplace equation is the diffusion equation with the infinite diffusion constant, the viscous fingering is the large diffusion limit of the crystal growth.

A new example of boundary dynamics is presented by a simple experiment of Yamazaki and Mizuguchi[5]; The mixture of water and corn starch powder is sandwiched between two glass plates. After a several hours, a labyrinthine pattern of dried corn starch will be formed when the water is evaporated from the gap of the glass plates. The system is two-dimensional, and the pattern is formed by the water-air interface line as it sweeps the system to collect the granules along it by means of the surface tension. The grains are simply accumulated along the interface line to give friction against the interface motion, and eventually get stuck with the glass plates.

In the above experiment, the granules play an analogous role to that of the latent heat in the crystal growth; They are distributed in the wet (or melted) region, but show up when the interface passes; The interface speed is controlled by the granule density (or temperature) at the boundary. The difference is that the granules do not diffuse while the heat does. In this sense, this *sweeping dynamics* is the small diffusion limit of Mullins-Sekerka problem; That is the opposite limit to Saffman-Taylor problem but has not been investigated yet in detail.

Analogous instabilities exist for these phenomena; A protruded part of interface advances faster because the

generated heat diffuses faster (Mullins-Sekerka), the pressure gradient is larger (Saffman-Taylor), or the accumulated granules are diluted over the elongated interface at the convex region (sweeping dynamics).

Similarities is seen in the phase field model proposed for this sweeping phenomenon[6, 7]. The model consists of two fields: the phase field and the coupling field; The coupling field represents the granular density, instead of the temperature in the crystal growth[8, 9, 10]. It has been demonstrated the model is capable to reproduce some feature of the patterns obtained in the experiment[7].

In this paper, we will construct the model of the boundary dynamics for the sweeping interface based on geometrical and physical considerations, and study its behavior.

II. SYSTEM CONFIGURATION AND CO-ORDINATE

Let us start by defining the Cartesian coordinate in the two dimensional system near the interface between the swept (dry) and the unswept (wet) region as in Fig.1(a). In the unswept region, the granules are distributed at the area density ρ , which we assume constant in this paper, for simplicity.

Suppose that the interface position at the time t is

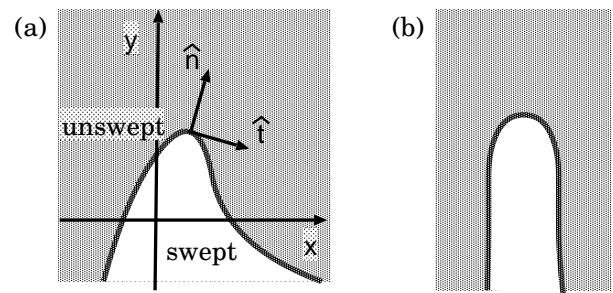


FIG. 1: Schematic diagram of the interface between the swept and the unswept regions. (a) Coordinate system with the normal and tangential vectors. (b) Steadily extending finger.

represented parametrically by

$$\mathbf{r}(t, s) = (x(t, s), y(t, s)) \quad (1)$$

with the parameter s . Let ℓ be the natural coordinate along the interface, then the length element $d\ell$ is

$$d\ell = \sqrt{(\partial x/\partial s)^2 + (\partial y/\partial s)^2} ds. \quad (2)$$

We define the tangential and the normal unit vectors of the interface, $\hat{\mathbf{t}}$ and $\hat{\mathbf{n}}$, by

$$\hat{\mathbf{t}} \equiv \partial \mathbf{r} / \partial \ell, \quad \hat{\mathbf{n}} \equiv \hat{\mathbf{z}} \times \hat{\mathbf{t}}, \quad (3)$$

where $\hat{\mathbf{z}}$ denotes the unit vector along the z axis perpendicular to the system; The normal vector $\hat{\mathbf{n}}$ is pointing into the unswept region. The curvature κ is defined as

$$\kappa \equiv -\frac{\partial \hat{\mathbf{t}}}{\partial \ell} \cdot \hat{\mathbf{n}}, \quad (4)$$

which is positive when the interface is convex toward the unswept side.

In the drying process, the interface moves upwards. Using an appropriate parameterization of s in Eq.(1), $\partial \mathbf{r} / \partial t$ can be made parallel to $\hat{\mathbf{n}}$, then the normal speed of the interface motion v_n is defined by

$$\frac{\partial \mathbf{r}(t, s)}{\partial t} = v_n(t, s) \hat{\mathbf{n}}(t, s). \quad (5)$$

III. DYNAMICS OF SWEEPING INTERFACE

We now consider the sweeping dynamics where the granules are swept by the interface; They are accumulated along the interface and conveyed by it in its normal direction. If we ignore the width of the region where the granules are accumulated, then the accumulated granules are described by the line density σ along the interface.

In the case where the granules are simply accumulated along the interface and do not diffuse at all, the equation for σ is determined geometrically and should be given by

$$\frac{\partial \sigma(t, s)}{\partial t} = v_n(t, s) \left[\rho - \kappa(t, s) \sigma(t, s) \right]. \quad (6)$$

The first term of the right hand side simply represents the sweeping accumulation. The second term comes from the change of the interface length as it advances; The length element along the interface increases by the factor $(1 + \kappa v_n \Delta t)$ during the short time period Δt , thus the line density decreases by the factor of its inverse.

The interface speed v_n , on the other hand, is given by the product of the following two factors, i.e. the driving force to the interface, and the mobility of the interface; (i) The driving force comes from the pressure difference ΔP between the wet and the dry regions; As the water evaporates, the volume of the wet region tends to shrink,

then the interface recedes due to the pressure difference. When the interface is curved, the driving force is given by the effective pressure difference $(\Delta P - \gamma \kappa)$ with γ being the surface tension, thus is proportional to the factor $(1 - a\kappa)$ with the capillary length $a \equiv \gamma / \Delta P$. (ii) The mobility depends upon the granule density σ and should be a decreasing function of it because the granule friction with the glass plates resists the interface motion. The mobility becomes zero at σ_{st} when the interface gets stuck with granules.

In the simplest case where no other scales of σ are involved, we can write down the equation for the interface speed as

$$v_n = v_0 f(\sigma / \sigma_{st}) (1 - a\kappa) \quad (7)$$

with the characteristic speed v_0 and the dimensionless mobility $f(x)$, which is a decreasing function with $f(0) = 1$ and $f(1) = 0$.

Eqs.(6) and (7) define the boundary dynamics of the sweeping interface, which shows morphological instability analogous to the crystal growth dynamics; The part of the interface with $\kappa > 0$ tends to advance faster when $f' < 0$.

The model contains four parameters, ρ , v_0 , σ_{st} , and a , from which we can define the stuck-in distance ℓ_{st} and the stuck-in time t_{st} by

$$\ell_{st} \equiv \sigma_{st} / \rho, \quad t_{st} \equiv \ell_{st} / v_0, \quad (8)$$

which are the distance and the time that the flat interface can advance before it gets stuck.

In order to simplify the expressions, in the following, we employ the dimensionless unit system where $\ell_{st} = t_{st} = \sigma_{st} = 1$, then Eqs.(6) and (7) are in the form of

$$\frac{\partial \sigma(t, s)}{\partial t} = v_n(t, s) \left[1 - \kappa(t, s) \sigma(t, s) \right], \quad (9)$$

$$v_n(t, s) = f(\sigma(t, s)) (1 - R\kappa(t, s)), \quad (10)$$

with the only one dimensionless parameter

$$R \equiv a / \ell_{st} = a\rho / \sigma_{st}. \quad (11)$$

This is the ratio of the capillary length to the stuck-in distance and is a measure of the effect of the surface tension.

The functional form of the dimensionless mobility $f(\sigma)$ in Eq.(10) should reflect the physical mechanism how the interface slows down and gets stuck due to the accumulated granules. Here, we employ the simplest form

$$f(\sigma) = \begin{cases} (1 - \sigma) & \text{for } 0 \leq \sigma \leq 1 \\ 0 & \text{for } \sigma > 1 \end{cases}. \quad (12)$$

IV. SIMPLE SOLUTIONS

Now, we study the interface dynamics based on Eqs.(9),(10), and (12).

A. flat interface

For the flat interface, $\kappa = 0$, thus the solution is easily obtained as

$$v_n(t) = e^{-t} \equiv v_f(t), \quad \sigma(t) = 1 - e^{-t} \equiv \sigma_f(t). \quad (13)$$

The flat interface can advance only by $\ell_{st}(=1)$ before it gets stuck because it simply accumulates material.

B. steadily extending finger

A possible mode of steady advance is the extending one-dimensional finger of the width of $2\ell_{st}$ by shoving the granules asides(Fig.1(b)).

This type of steadily extending finger solution can be obtained as follows. Suppose the finger is extending in the y direction with the speed V , then Eqs.(9) and (10) become

$$-V\sigma'y' = (1 - \kappa\sigma)Vx', \quad (14)$$

$$Vx' = (1 - \sigma)(1 - R\kappa), \quad (15)$$

where the primes denote the derivative by the natural coordinate ℓ . Then, x' and y' are related as

$$x'^2 + y'^2 = 1, \quad (16)$$

thus, Eqs. (14) – (16) can be solved for x , y , and σ as functions of ℓ under the physical boundary conditions

$$\begin{aligned} (x, y) &= (0, 0) \quad \text{at} \quad \ell = 0 \\ (x, y) &= (\mp 1, -\infty), \quad \sigma = 1 \quad \text{at} \quad \ell = \pm\infty, \end{aligned}$$

for a given set of R and V .

For a given R , a steady solution is possible for a finite range of V ; The condition at the tip that $x' = 1$ and $y' = 0$ at $\ell = 0$ in Eqs.(14) and (15) leads to the allowed range of V ,

$$V \leq (1 - \sqrt{R})^2. \quad (17)$$

Eqs.(14)–(16) can be solved numerically. Fig.2 shows some of the steady solutions for the finger shape and the line density σ for $R = 0.2$ with $V = 0.1, 0.2$, and 0.3 . One can see that the finger tip is sharper for the larger extending speed V .

The line density σ shows rather intriguing behavior as a function of ℓ ; The tip density is smaller for the larger V , but for V larger than a certain value for a given R , σ becomes singular at the tip and eventually develops a cusp. Actually, by expanding σ around the tip, it can be shown that σ becomes non-analytic

$$\sigma(\ell) - \sigma(0) \propto \ell^\varphi \quad (18)$$

with

$$\varphi = \frac{2\sqrt{(1 - V + R)^2 - 4R}}{(1 - V - R) - \sqrt{(1 - V + R)^2 - 4R}} \quad (19)$$

when

$$1 + \frac{1}{3} \left[5R - 4\sqrt{R^2 + 3R} \right] < V < (1 - \sqrt{R})^2. \quad (20)$$

The singularity at the tip in the line density is a peculiar result of the model without diffusion.

V. ULTRA-VIOLET CATASTROPHE IN THE DIFFUSIONLESS MODEL

We have derived the steady finger solutions, which are smooth and analytic except at the finger tip, but in a general time development, the diffusionless feature of the model seems to cause the ultra-violet catastrophe, or the short wave length instability, even though we have taken account of the surface tension effect by introducing the capillary length.

Actually, numerical simulations of the equations eventually yield a zigzag structure of the solution in the shortest discretization length; This cannot be accepted as a solution of the differential equations.

Mathematically, the problem is that the surface tension effect in eq.(10) is of the same form as κ with the term that causes the instability in eq.(9), thus the surface tension effect never dominates to suppress the instability even in the short wave length limit, unlike in the case of Mullines-Sekerka/Saffman-Taylor problems.

This may be seen in the linear stability analysis of the flat interface solution (13)[11]. Since the flat interface solution is not steady, the linearized equations for the small deviation from it are not of constant coefficient, thus the analysis is not simple, but within the approximation where the time variation is neglected during the

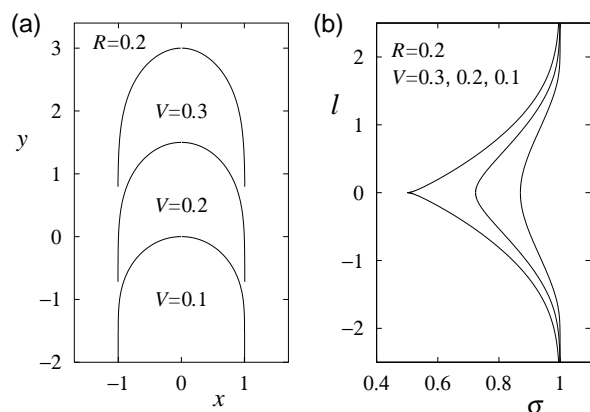


FIG. 2: Steadily propagating finger solutions without diffusion for $R = 0.2$ with $V = 0.3, 0.2$, and 0.1 . (a) Shapes of the finger. The plots for different speeds are shifted to avoid overlapping. Only the part near the tip is shown for each finger. (b) The line density of granules v.s. ℓ . The finger tip is located at $\ell = 0$.

time scale of the perturbation (quasi-steady approximation), the growth rate $\Omega(q)$ of the unstable perturbation with the wave number q in the unstable branch can be obtained as

$$\Omega(q) = \frac{1}{2} \left[-(Rv_f q^2 - f'_f) + \sqrt{(Rv_f q^2 - f'_f)^2 - 4f'_f \sigma_f v_f q^2} \right], \quad (21)$$

where $f'_f = f'(\sigma_f(t))$; v_f and σ_f are given by eq.(13). This is positive for any $q > 0$ when $f'_f < 0$ and

$$\Omega(q) \rightarrow -\frac{f'_f \sigma_f}{R} \quad \text{for } q \rightarrow \infty, \quad (22)$$

suggesting the ultra-violet catastrophe, thus the model is not well defined in the continuum limit.

VI. DIFFUSION DRIVEN BY INTERFACE MOTION

In order to avoid this instability, we introduce the diffusion term along the interface in Eq.(9) as

$$\frac{\partial \sigma}{\partial t} = v_n \left[1 - \kappa \sigma \right] + \frac{\partial}{\partial \ell} \left(\ell_D v_n \frac{\partial \sigma}{\partial \ell} \right) \quad (23)$$

with a new small length scale ℓ_D . The adopted form represents the diffusion flux along the interface; The flux is proportional to the interface speed v_n . Such a diffusion flux is natural in the case where the diffusion is driven by the interface motion; The grains are driven randomly along the interface by the distance ℓ_D during the time ℓ_D/v_n , i.e. the time during which the interface moves by ℓ_D in the normal direction. Note that we do not assume the diffusion perpendicular to the interface.

The linear stability analysis within the same approximation as above gives the perturbation growth rate

$$\Omega(q) = \frac{1}{2} \left[-\left((R + \ell_D) v_f q^2 - f'_f \right) + \sqrt{\left((R + \ell_D) v_f q^2 - f'_f \right)^2 + 4 \left((-f'_f) \sigma_f - \ell_D R v_f q^2 \right) v_f q^2} \right], \quad (24)$$

which gives

$$\Omega(q) < 0 \quad \text{for } q > q_s \equiv \sqrt{\frac{(-f'_f) \sigma_f}{\ell_D R v_f}}, \quad (25)$$

therefore the catastrophe is suppressed.

VII. NUMERICAL SIMULATION OF FINGER SOLUTIONS

I have performed simulations on the model with this diffusion in order to see if the finger solutions are stable.

Let us start by examining the effect of the length scale ℓ_D . Fig.3 shows the results of simulations of Eqs.(10) and

(23) for $R = 0.2$ with $\ell_D = 0.2, 0.1,$ and 0.05 . The steady solution of $V = 0.1$ without the diffusion ($\ell_D = 0$) is used as the initial state. Only the right halves of the interfaces are shown and the time development is represented by the plots with the time interval $\Delta t = 1$. I have confirmed the ultra-violet catastrophe is suppressed by the diffusion term; Except for the cusps at the edges of sticking regions, numerical solutions converges to a smooth solution as the smaller time and space discretization is used for integral in contrast with the diffusionless model, where the zigzag structure in the smallest discretization scale develops eventually all over the interface due to the ultra-violet catastrophe. In all cases of Fig.3, the fingers extend at a speed of 0.1 initially with keeping the initial shape as the steady solution does, but eventually the finger becomes unstable and develops wavy structures. The length scale of the emerging structure is shorter for the smaller ℓ_D , but they are much larger than ℓ_D . We do not see any tendency that the steady solution becomes stable for small ℓ_D even though the initial configuration of the steady solution for the speed $V = 0.1$ with $R = 0.2$ is outside the range Eq.(20), thus does not have a singularity in σ at the tip.

Fig.4 shows the results for the case of $R = 0.2$ and $\ell_D = 0.1$. The initial states are the steady solutions of $V = 0.1, 0.2,$ and 0.3 for $\ell_D = 0$. One may see some differences in the way how the steady solutions are destabilized for different speeds, but again the steady solutions are unstable for all the cases, and complex developments of the boundary are seen after the instability.

The unstable development seen in Figs.3 and 4 shows some similarities to the pattern found in [5]; Concave parts of the interface evolve eventually into cusps with the tip size of ℓ_D , and the interface are pinned by them. This leads to the irregular development of the interface although there is no randomness in the present model.

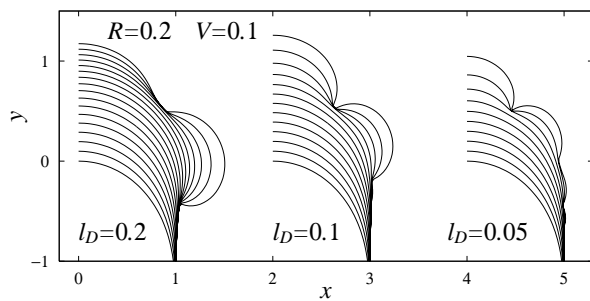


FIG. 3: The time developments of the interface for $R = 0.2$ with $\ell_D = 0.2, 0.1,$ and 0.05 . Only the right halves of the fingers are shown. The time sequences are shown with the time interval $\Delta t = 1$. The steady solution for $V = 0.1$ with $\ell_D = 0$ are used as the initial configurations for all the cases.

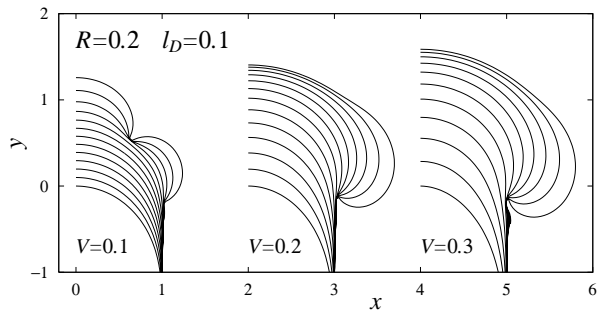


FIG. 4: The time developments of the interface for $R = 0.2$ and $\ell_D = 0.1$ from some initial configurations. The steady solutions of the speed $V = 0.1, 0.2,$ and 0.3 with $\ell_D = 0$ are used as the initial configurations. The time sequences are shown with the time interval $\Delta t = 1$.

VIII. CONCLUDING REMARKS

Before concluding, let us make some remarks.

First of all, the sweeping phenomena can be seen commonly; It is not limited to the specific experiment we referred to, although there have not been many controlled experiments and theoretical analyses. Another example may be found in a pattern formation of deposit in a drying droplet[12]. Actual situations varies and may not be as simple as the one we have analyzed in this paper, but there should be a class of phenomena characterized by the sweeping phenomenon as is discussed here.

Secondly, the boundary dynamics should be able to be derived from the phase field model as the narrow interface width limit. In the case of crystal growth and the viscous fingering, the interface width is the shortest length scale in the problem, and the boundary dynamics can be derived from the phase field model by taking ap-

propriate limits[13]. On the other hand, in the sweeping phenomenon, the length scale over which the granular density varies in the normal direction to the interface is in the same order with the interface width[7], which complicates the formal derivation of the boundary dynamics.

Lastly, some comments on the diffusion are in order. We have formulated the sweeping dynamics as the small diffusion limit, but in a real system, some form of diffusion should exist. We have also found that the diffusionless model shows the short wave instability. In Ref.[7], the ordinary diffusion is assumed within the interface, which results in patterns with a larger scale for a slower process; This does not seem to agree with the experiment. On the other hand, we regularized the model with the diffusion characterized by the short length scale ℓ_D , which may correspond to the grain size in the experiment[5]. The diffusion along the interface is considered to be driven by the interface motion, thus the grains do not diffuse when the interface gets stuck, therefore, the slower interface motion does not lead to a larger scale.

In summary, the boundary dynamics of the sweeping interface is constructed based upon geometrical and physical analysis of the process. To suppress the short length scale instability, the diffusion driven by the interface motion along the interface is introduced with the short length scale ℓ_D . In the case of no diffusion, we obtain the steadily propagating finger solutions for a finite range of propagation speed, but the numerical simulations with the small diffusion suggests that they are unstable, and a complex behavior of the interface is seen.

Acknowledgments

This work is supported by Grant-in-Aid for Scientific Research (C) (No. 16540344) from JSPS, Japan.

-
- [1] For review, see for example, J.S. Langer, *Rev. Mod. Phys.* **52**, 1 (1980).
 - [2] W.W. Mullins and R.F. Sekerka, *J. Appl. Phys.* **34**, 323 (1963); *ibid.* **35**, 444 (1964).
 - [3] For review, see for example, D. Bensimon, L.P. Kadanoff, S. Liang, B.I. Shraiman, and C. Tang, *Rev. Mod. Phys.* **58**, 977 (1986).
 - [4] P.G. Saffinan and G. Taylor, *Proc. R. Soc. London, Ser. A* **245**, 312 (1958).
 - [5] Y. Yamazaki and T. Mizuguchi, *J. Phys. Soc. Jpn.* **69**, 2387 (2000).
 - [6] Y. Yamazaki, M. Mimura, T. Watanabe, and T. Mizuguchi, unpublished.
 - [7] T. Iwashita, Y. Hayase, and H. Nakanishi, *J. Phys. Soc. Jpn.* **74**, 1657 (2005).
 - [8] J.S. Langer, in "Directions in condensed matter physics" edited by G. Grinstein and G. Mazenko (World Scientific, 1986) pp. 165–186.
 - [9] O. Penrose and P.C. Fife, *Physica D* **43**, 44 (1990).
 - [10] R. Kobayashi, *Physica D* **63**, 410 (1993)
 - [11] J. Krug, private communication.
 - [12] R.D. Deegan, *Phys. Rev. E* **61**, 475 (2000).
 - [13] G. Caginalp, *Phys. Rev. A* **39**, 5887 (1989).